CONFIDENTIAL

NACA RESEARCH MEMORANDUM

WIND-TUNNEL INVESTIGATION AT LOW SPEED OF THE EFFECT OF VARYING THE RATIO OF BODY DIAMETER TO WING SPAN FROM 0.1 TO 0.8 ON THE AERODYNAMIC CHARACTERISTICS IN PITCH OF A 45° SWEPTBACK-WING—BODY COMBINATION

By Harold S. Johnson

Langley Aeronautical Laboratory
Langley Field, Va.

NATIONAL ADVISORY COMMITTEE
FOR AERONAUTICS

WASHINGTON

November 30, 1953

CONFIDENTIAL

NATIONAL ADVISORY COMMITTEE FOR AERONAUTICS

RESEARCH MEMORANDUM

WIND-TUNNEL INVESTIGATION AT LOW SPEED OF THE EFFECT OF VARYING THE RATIO OF BODY DIAMETER TO WING SPAN FROM 0.1 TO 0.8 ON THE AERODYNAMIC CHARACTERISTICS IN PITCH OF A 45° SWEPTBACK-WING—BODY COMBINATION

By Harold S. Johnson

SUMMARY

Force and moment data were obtained at low speed for a family of bodies and wing-body combinations to determine the effects of varying the ratio of body diameter to wing span from 0.1 to 0.8 on the aerodynamic characteristics in pitch. The bodies had $1\frac{1}{2}$-caliber ogival noses and cylindrical afterbodies. The untapered 45° sweptback wings had aspect ratios of 3 and NACA 65A006 airfoil sections parallel to the body center line. Lift, drag, and pitching-moment data were obtained through a -6° to about 40° angle-of-attack range. In addition, the experimental lift characteristics of the body alone and the wing-body combination were compared with several existing theories.

There was a linear increase in lift-curve slope at 0° angle of attack with body-diameter—wing-span ratio D/b for the $D/b = 0.1$ to 0.4 range, and further increases in D/b from 0.4 to 0.8 resulted in only slight changes in the lift-curve slope. The lift-curve slope as estimated by an approximate theory was in excellent agreement with experiment for the D/b range investigated. The body-alone lift coefficient (based on the maximum cross-sectional area of the body) at a given angle of attack increased with the body fineness ratio for the 4.5- to 7.5-fineness-ratio range investigated.

INTRODUCTION

Since the advent of supersonic flight, more radical departures from conventional airplane configurations have been made or are being considered. The rapid development of guided missiles has indicated that

even more extreme configurations show promise of providing satisfactory supersonic flight characteristics. One of the basic airplane design variables that is being altered by the demands of increased speeds is the ratio of fuselage diameter to wing span. The combination of low-aspect-ratio wings and a decrease in the wing area required has resulted in ratios of fuselage diameter to wing span of as high as about 0.5. Thus, the determination of mutual interference between a wing and a body has become more important. Therefore, both experimental data and theoretical studies of the forces and moments mutually induced by a wing and a body are of appreciable interest.

Recent studies (for example, refs. 1 to 6) have provided information on this interference effect and show the great variety of problems involved as well as methods so far employed in dealing with them.

Reported herein are the results of an investigation made to determine the low-speed aerodynamic characteristics in pitch of a 45° sweptback-wing—body combination having a body-diameter—wing-span ratio range of 0.1 to 0.8 for a wide angle-of-attack range that extended well beyond the wing stall. In addition, theoretical estimates of the lift characteristics of the body alone and of the wing-body combination are compared with the experimental results.

COEFFICIENTS AND SYMBOLS

The results of the tests are presented as standard NACA coefficients of forces and moments about the stability axes (which for the conditions of these tests (0° yaw) correspond to the wind axes). The pitching-moment coefficients are given about the quarter-chord point of the mean aerodynamic chord shown in figure 1. The positive directions of forces and moment are shown in figure 2.

A	aspect ratio, b^2/S
A_E	aspect ratio of exposed wing, $(b - D)^2/S_E$
b	wing span, 1.458 and 2.917 ft
$\bar{c}$	wing mean aerodynamic chord, 0.486 and 0.972 ft
D	maximum body diameter, ft
l	length of body, ft
q	free-stream dynamic pressure, $\frac{1}{2}\rho V^2$, lb/sq ft

S_B maximum cross-sectional area of body, sq ft

S_E exposed wing area, sq ft

S_w wing area, 0.709 and 2.836 sq ft

V free-stream velocity, ft/sec

α angle of attack, deg

ρ mass density of air, slugs/cu ft

C_L lift coefficient based on wing geometry, $\frac{\text{Lift}}{qS_w}$

C_{L_B} lift coefficient of body based on body geometry, $\frac{\text{Lift}}{qS_B}$

$C_{L_\alpha} = \frac{\partial C_L}{\partial \alpha}$ at $\alpha = 0^\circ$

$C_{L_{\alpha_B}} = \frac{\partial C_{L_B}}{\partial \alpha}$ at $\alpha = 0^\circ$

C_D drag coefficient based on wing geometry, $\frac{\text{Drag}}{qS_w}$

C_{D_B} drag coefficient of body based on body geometry, $\frac{\text{Drag}}{qS_B}$

C_m pitching-moment coefficient based on wing geometry,

$$\frac{\text{Pitching moment}}{qS_w\bar{c}}$$

C_{m_B} pitching-moment coefficient of body based on body geometry,

$$\frac{\text{Pitching moment}}{qS_B l}$$

Subscripts:

L	large wing
S	small wing

The abbreviation F.R. is used for fineness ratio.

MODEL AND APPARATUS

The bodies and wing-body combinations were tested in the Langley 300 MPH 7- by 10-foot tunnel by utilizing a sting-support system (fig. 3) and an electrical strain-gage balance contained within the body. In order to provide the desired range of body-diameter—wing-span ratio $\left(\frac{D}{b} = 0.1 \text{ to } 0.8\right)$, two wings, having spans of 17.5 inches (referred to as the small wing) and 35.0 inches (large wing), were tested in combination with four bodies having diameters of 3.5, 7.0, 10.5, and 14.0 inches. Both wings were untapered and had 45° of sweepback, aspect ratios of 3.00, and NACA 65A006 airfoil sections parallel to the plane of symmetry. The bodies had ogival noses of $1\frac{1}{2}$ calibers and cylindrical afterbodies. Because of mounting limitations (the body length had to be long enough to contain the balance and short enough to clear the mounting strut), the body fineness ratios varied from 4.5 to 7.5. (See fig. 1(c).) The 7.0-inch-diameter body and wing-body configurations were tested at fineness ratios of both 5.0 and 7.0. The wing-chord plane was coincident with the horizontal plane of symmetry of the body. Drawings of the configurations investigated are shown in figure 1.

TESTS

The tests were made in the Langley 300 MPH 7- by 10-foot tunnel at dynamic pressures of approximately 30 and 120 lb/sq ft for the configurations having the large wing and the small wing, respectively. Body-alone tests were made at both of these dynamic pressures. The corresponding Mach numbers were 0.14 and 0.29, and the Reynolds number was about 0.9×10^6 based on the wing mean aerodynamic chords. Lift, drag, and pitching-moment data were obtained for an angle-of-attack range of about -6° to about 40° unless this range was limited by model load or extreme vibration.

CORRECTIONS

The angle-of-attack values have been corrected to account for the deflection of the balance and support strut under load. Jet-boundary corrections, computed by the method outlined in reference 7, were applied to the data. Blockage corrections have been applied to the data according to the method of reference 8. Buoyancy corrections have been applied to account for the longitudinal static-pressure gradient in the tunnel.

RESULTS AND DISCUSSION

Presentation of Data

The body-alone aerodynamic characteristics are presented in figure 4 and the effect of body fineness ratio for the 7.0-inch-diameter body-alone configuration is shown in figure 5. A comparison between the experimentally and theoretically determined variation of $C_{L_{\alpha_B}}$ with body fineness ratio is shown in figure 6.

The aerodynamic coefficients of the wing-body configurations are presented in figure 7, and the effect of body fineness ratio for the wing-body combinations having the 7.0-inch-diameter body is shown in figure 8. The $D/b = 0.2$ and 0.4 wing-body configurations having the large wing are compared with the same configurations having the small wing in figure 9. The experimentally determined variation of lift-curve slope at $\alpha = 0^\circ$ with D/b is compared with theory in figure 10. The theoretical ratio of induced body lift to wing lift as determined from reference 4 or 9 is shown in figure 11. The various contributions to the theoretically determined lift of the wing-body configuration are presented in figure 12 as a function of D/b.

Body-Alone Characteristics

Lift.- The variation of lift coefficient (based on the body geometry) with angle of attack was similar for the four sizes of bodies investigated and the data exhibited consistent effects of variations in both body fineness ratio and dynamic pressure (figs. 4(a), 5(a), and 6). At a given angle of attack, the lift coefficient increased with body fineness ratio for the 4.5- to 7.5-fineness-ratio range investigated. A change in dynamic pressure from about 30 lb/sq ft to about 120 lb/sq ft had a negligible effect on the lift data for angles of attack of less than about 16°. For a given angle of attack greater than about 16°, the lift coefficient was greater at the higher dynamic pressure and the change

in C_{L_B} was generally greater for the bodies having the higher fineness-ratio values. The lift-curve slope did not vary with α for angles of attack of less than about 12° to 16°. At angles of attack greater than about 16°, the lift-curve slope was greater than that for values of α of less than about 16°, and larger increases in slope at the high values of α were noted for the bodies having the higher values of body fineness ratio (figs. 4(a) and 5(a)). There was no indication of body stalling below $\alpha = 40°$.

For the 4.5- to 7.5-fineness-ratio range investigated, the lift-curve slope at $\alpha = 0°$ $C_{L_{\alpha_B}}$ increased very nearly linearly with body fineness ratio as shown in figure 6 and table I. Also presented in figure 6 are the theoretical $C_{L_{\alpha_B}}$ values determined by the methods of references 4 and 10. As determined by the method of reference 4, the lift is a function only of angle of attack and base area and is independent of the body fineness ratio ($C_L = 2\alpha$ where α is expressed in radians and the reference area is the base area of the body). It should be noted that this theory may underestimate the lift for bodies that have a base area less than the maximum cross-sectional area since viscosity effects may be present and the effective base area of such bodies will be larger than the actual base area by an amount dependent on the thickness of the boundary layer (ref. 4). In the method of reference 10, this 2α term is reduced by a factor to approximate the effects of body fineness ratio. The method of reference 10 also includes a nonlinear α^2 term to approximate the effects of the viscous cross flow. For the bodies investigated, this theory considerably overestimated the increase in lift-curve slope with α, but the computed increment of C_{L_B} resulting from a change in body fineness ratio is in good agreement with the experimental results.

Drag.- The effects of changes in both body fineness ratio and dynamic pressure on the drag characteristics were generally similar to those on the lift data (figs. 4(a) and 5(a)). At a given angle of attack, the drag coefficient increased as the body fineness ratio was increased for the 5.0 to 7.0 range investigated and this change in C_{D_B} increased with angle of attack (fig. 5(a)). The change in dynamic pressure from about 30 lb/sq ft to about 120 lb/sq ft resulted in negligible changes in C_{D_B} for angles of attack of less than about 20° and increases in C_{D_B} for angles of attack greater than about 20°. This increase in C_{D_B} at high values of α was most pronounced for the bodies having the higher fineness ratios.

Pitching moment.- A direct comparison of the pitching-moment data for the various bodies tested cannot be made in figure 4(a) since the

body fineness ratios and the moment-center locations varied (fig. 1). The experimental results for the two bodies having fineness ratios of 5.0 (D = 7.0 in. and 10.5 in.) were in substantial agreement when referred to the same moment center. As expected, an increase in afterbody length of 2 diameters had a stabilizing effect throughout the angle-of-attack range investigated (fig. 5(a)).

Wing-Body Characteristics

Lift.- For values of α of less than about 12°, the data of figures 7 and 8 show that the lift-curve slope generally increased with α and that this change in lift-curve slope with α increased with D/b for the 0.1 to 0.6 D/b range. For this angle-of-attack range, the lift-curve-slope values for the D/b = 0.8 configuration were slightly less than those for the D/b = 0.6 configuration. As the ratio of body diameter to wing span was increased, the effect of the wing stall generally became less pronounced. For angles of attack above the wing stall ($\alpha \approx 20°$), the lift coefficient of the D/b = 0.1 configuration was relatively unaffected by changes in α. For this high angle-of-attack range, the lift coefficient at a given angle of attack increased as the D/b ratio was increased as a result of both increasing body lift with α for angles of attack beyond the wing stall and induced effects.

The lift coefficient at a given angle of attack was increased by a change in body fineness ratio from 5.0 to 7.0 for the D/b = 0.2 and 0.4 configurations (fig. 8). This increase in C_L with fineness ratio was of about the same magnitude as was noted for the body-alone configurations based on the corresponding wing areas (figs. 5(b) and 5(c)). The increment of lift coefficient resulting from the change in body fineness ratio increased very nearly linearly with α. The lift data for the D/b = 0.2 and 0.4 configurations having the large wing are in very good agreement with those for the same configurations having the small wing when the effect of the one-half-caliber difference in body fineness ratio is considered (fig. 9).

The experimentally determined lift-curve slopes for the various wing-body combinations at $\alpha = 0°$ are given in table I and are presented in figure 10 approximately adjusted (by using the experimental body-alone and wing-body data) to body fineness ratios of 5.0 and 7.0 where necessary. A linear increase in C_{L_α} with D/b is shown for the D/b = 0.1 to 0.4 range, and further increases in D/b from 0.4 to 0.8 resulted in only slight changes in C_{L_α}. The lift-curve slope for D/b = 1.0 (obtained from the body-alone data with the lift coefficient based on the area of a hypothetical untapered aspect-ratio-3 wing) was appreciably higher than that for the D/b = 0.8 configuration. The C_{L_α} values computed by the method of reference 1 are in excellent agreement with

the experimentally determined values (fig. 10). In this method, the lift of a wing-body combination is considered to be the summation of four contributions: lift of the exposed wing, body lift, induced wing lift (resulting from the body upwash flow field), and the induced body lift (resulting from the wing flow field). The lift of the exposed wing is approximated by assuming that the fuselage acts as an infinite end plate $\left(A_E = (b - D)^2/S_E\right)$. In the calculations presented in this paper, the lift-curve slope of the exposed wing was computed by the following equation[1]:

$$C_{L_\alpha} = \frac{A_E/57.3}{\frac{1}{\pi} + \sqrt{\left(\frac{1}{\pi}\right)^2 + \left(\frac{A_E}{a_o \cos \Lambda}\right)^2 - \left(\frac{A_E M}{a_o}\right)^2}}$$

where a_o is the section lift-curve slope per radian, Λ is the sweep of the 50-percent-chord line in degrees, and M is the Mach number. The induced wing lift is approximated by increasing the wing angle of attack by the average upwash angle over the exposed span of the wing as determined by potential theory (refs. 11 or 12). This average upwash angle is shown to be equal to $(D/b)\alpha$ and the effective angle of attack of the exposed wing is therefore $(1 + D/b)\alpha$. The induced body lift (resulting from the upwash flow field ahead of the wing, the downwash behind the wing, and the loading carried over the body in the vicinity of the wing) is approximated by assuming this lift to have the same relationship to the lift of the wing in the presence of the body as that for a configuration having a wing mounted on a cylinder of infinite length (refs. 4 or 9). This ratio of induced body lift to wing lift is shown in figure 11 as a function of D/b. The variation of these four contributions to the lift of the wing-body configuration investigated with D/b is shown in figure 12 with the body lift computed by the methods of references 4 and 10. Also shown in figure 12 is the change in lift resulting from a reduction of the body upwash to account for the effect of the finite wing thickness. The increment of wing lift resulting from the body upwash field was reduced by the ratio of body cross-sectional area above and below the wing to the cross-sectional area of the body. (See ref. 5.)

---

[1]This equation was derived by Mr. Edward C. Polhamus of the Langley Aeronautical Laboratory and was presented (in modified form) in unpublished lecture notes which were distributed at the Wright Field Seminar on Compressibility Effects on Aircraft Design, 1950. The derivation of this equation is similar to the lift-curve equation of reference 13 and gives results that are in excellent agreement with experimental results for wings having a wide range of plan forms.

Calculations were also made and good agreement with the experimental C_{L_α} values was obtained by using the method of reference 1 for the wing-body combinations of references 2, 14, and 15 (tapered unswept wing, tapered sweptback wings, and delta wing, respectively) and for the lift of the wing in the presence of the bodies for the configurations of reference 2. The methods of references 2 to 5 were not used because they either do not apply to the configurations of the subject investigation or require considerable modifications to account for the blunt bodies and large D/b values investigated.

Drag.- At a given angle of attack, the drag coefficient increased as the ratio of body diameter to wing span was increased (fig. 7). The drag coefficient at a given angle of attack was increased by a change in body fineness ratio of from 5.0 to 7.0 for both the $D/b = 0.2$ and 0.4 wing-body combinations (fig. 8).

Pitching moment.- For the wing-body combinations having body fineness ratios of 5.0, the instability increased with D/b (fig. 7). In general, an increase in afterbody length resulted in a reduction in the instability (figs. 7 and 8). There were large stabilizing changes in the pitching-moment slopes dC_m/dC_L resulting from the addition of the wing to the body (figs. 4(b), 4(c), and 7).

CONCLUSIONS

A wind-tunnel investigation was made at low speed to determine the effects of varying the ratio of body diameter to wing span D/b from 0.1 to 0.8 on the aerodynamic characteristics in pitch of a wing-body combination having an untapered 45° sweptback wing of aspect ratio 3 and a body having an ogival nose and a cylindrical afterbody. The results of the investigation led to the following conclusions:

1. There was a linear increase in lift-curve slope at 0° angle of attack with D/b for the $D/b = 0.1$ to 0.4 range and further increases in D/b from 0.4 to 0.8 resulted in only slight changes in the lift-curve slope.

2. Lift-curve-slope values near 0° angle of attack estimated by an approximate theory were in excellent agreement with the experimental results.

3. At a given angle of attack, the body-alone lift coefficient (based on the maximum cross-sectional area of the body) increased with body fineness ratio for the 4.5- to 7.5-fineness-ratio range investigated.

Langley Aeronautical Laboratory,
National Advisory Committee for Aeronautics,
Langley Field, Va., October 5, 1953.

REFERENCES

1. Flax, A. H., and Lawrence, H. R.: The Aerodynamics of Low-Aspect-Ratio Wings and Wing-Body Combinations. Rep. No. CAL-37, Cornell Aero. Lab., Inc., Sept. 1951.

2. Hopkins, Edward J., and Carel, Hubert C.: Experimental and Theoretical Study of the Effects of Body Size on the Aerodynamic Characteristics of an Aspect Ratio 3.0 Wing-Body Combination. NACA RM A51G24, 1951.

3. McLaughlin, Milton D.: Method of Estimating the Stick-Fixed Longitudinal Stability of Wing-Fuselage Configurations Having Unswept or Swept Wings. NACA RM L51J23, 1952.

4. Spreiter, John R.: The Aerodynamic Forces on Slender Plane- and Cruciform-Wing and Body Combinations. NACA Rep. 962, 1950. (Supersedes NACA TN's 1897 and 1662.)

5. Weber, J., Kirby, D. A., and Kettle, D. J.: An Extension of Multhopp's Method of Calculating the Spanwise Loading of Wing-Fuselage Combinations. Rep. No. Aero 2446, British R.A.E., Nov. 1951.

6. Lomax, Harvard, and Byrd, Paul F.: Theoretical Aerodynamic Characteristics of a Family of Slender Wing-Tail-Body Combinations. NACA TN 2554, 1951.

7. Gillis, Clarence L., Polhamus, Edward C., and Gray, Joseph L., Jr.: Charts for Determining Jet-Boundary Corrections for Complete Models in 7- by 10-Foot Closed Rectangular Wind Tunnels. NACA WR L-123, 1945. (Formerly NACA ARR L5G31.)

8. Herriot, John G.: Blockage Corrections for Three-Dimensional-Flow Closed-Throat Wind Tunnels, With Consideration of the Effect of Compressibility. NACA Rep. 995, 1950. (Supersedes NACA RM A7B28.)

9. Wieselsberger, C.: Airplane Body (Non Lifting System) Drag and Influence on Lifting System. Vol. IV of Aerodynamic Theory, div. K, Ch. III, sec. 1, W. F. Durand, ed., Julius Springer (Berlin), 1935, pp. 152-157.

10. Allen, H. Julian, and Perkins, Edward W.: Characteristics of Flow Over Inclined Bodies of Revolution. NACA RM A50L07, 1951.

11. Beskin, L.: Determination of Upwash Around a Body of Revolution at Supersonic Velocities. CVAC-DEVF Memo BB6, APL/JHU-CM-251, The Johns Hopkins Univ., Appl. Phys. Lab., May 27, 1946.

12. Glauert, H.: The Elements of Aerofoil and Airscrew Theory. Second ed., Cambridge Univ. Press, reprint of 1948, p. 30.

13. Diederich, Franklin W.: A Plan-Form Parameter for Correlating Certain Aerodynamic Characteristics of Swept Wings. NACA TN 2335, 1951.

14. Kuhn, Richard E., and Wiggins, James W.: Wind-Tunnel Investigation of the Aerodynamic Characteristics in Pitch of Wing-Fuselage Combinations at High Supersonic Speeds. Aspect-Ratio Series. NACA RM L52A29, 1952.

15. Riebe, John M.: The Effects of Fuselage Size on the Low-Speed Longitudinal Aerodynamic Characteristics of a Thin 60° Delta Wing With and Without a Double Slotted Flap. NACA RM L52L29a, 1953.

TABLE I

LIFT CHARACTERISTICS OF THE BODY ALONE AND WING-BODY COMBINATIONS

Body alone

D, in.	F.R.	$C_{L_{\alpha_B}}$ (a)	C_{L_α} (a b)	C_{L_α} (a c)
3.5	7.5	0.0350	0.0008	0.0033
7.0	5.0	.0319	.0030	.0120
7.0	7.0	.0340	.0032	.0128
10.5	5.0	.0320	.0068	.0271
14.0	4.5	.0317	.0119	.0477

[a]For $q \approx 30$ and 120 lb/sq ft.
[b]Based on S_w of large wing (b = 35.00 in.).
[c]Based on S_w of small wing (b = 17.50 in.).

Wing-Body Combinations

D, in.	b, in.	D/b	F.R.	C_{L_α} (d)
3.5	35.0	0.1	7.5	0.0525
7.0	35.0	.2	5.0	.0546
7.0	35.0	.2	7.0	.0550
10.5	35.0	.3	5.0	.0568
14.0	35.0	.4	4.5	.0583

[d]$q \approx 30$ lb/sq ft

D, in.	b, in.	D/b	F.R.	C_{L_α} (e)
3.5	17.5	0.2	7.5	0.0555
7.0	17.5	.4	5.0	.0590
7.0	17.5	.4	7.0	.0598
10.5	17.5	.6	5.0	.0595
14.0	17.5	.8	4.5	.0585

[e]$q \approx 120$ lb/sq ft

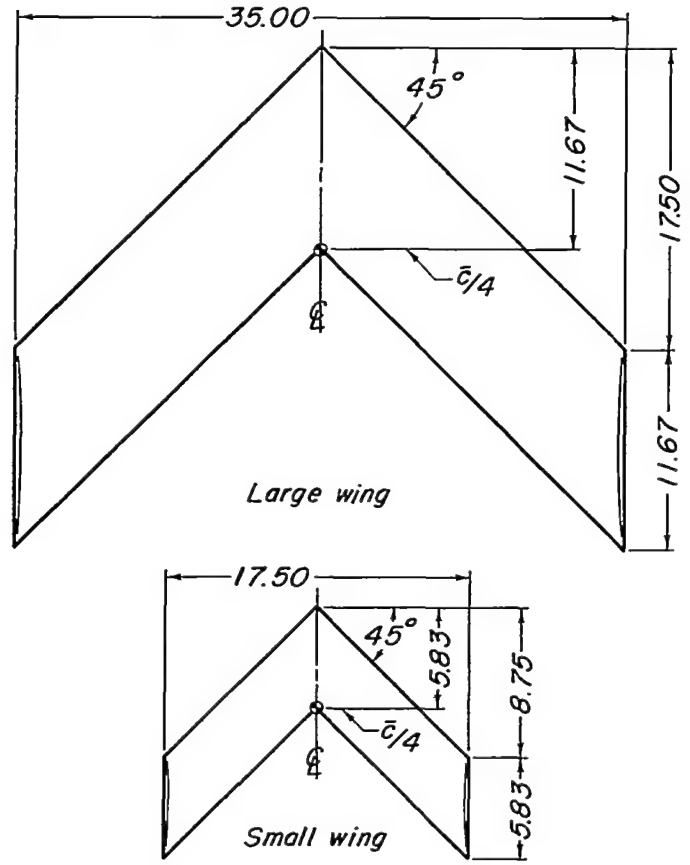

(a) Wings.

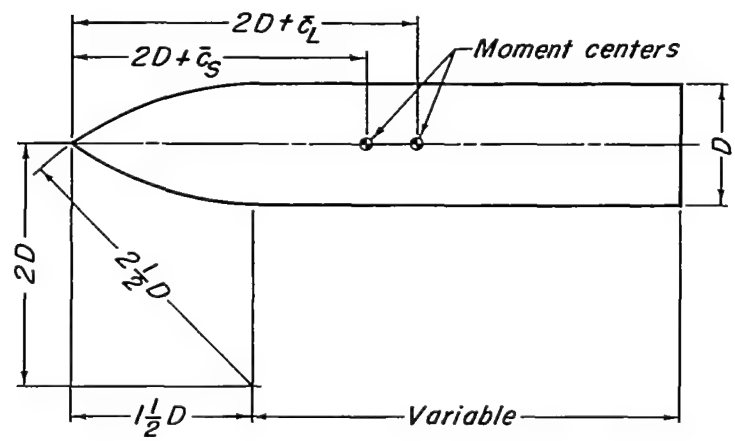

(b) Bodies.

Figure 1.- Dimensional characteristics of the wings, bodies, and wing-body combinations. Unless otherwise noted, all dimensions are in inches.

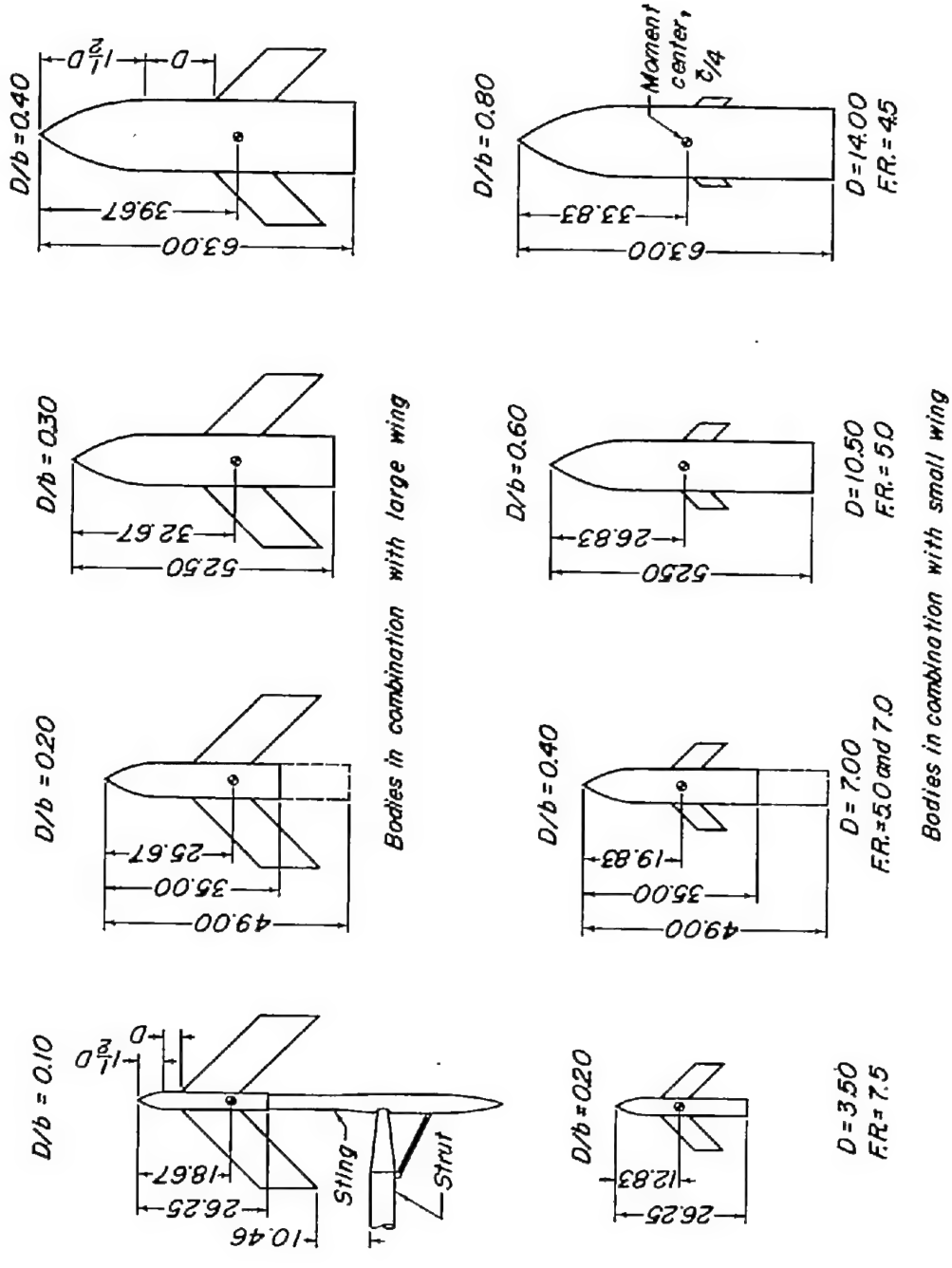

(c) Wing-body combinations.

Figure 1.- Concluded.

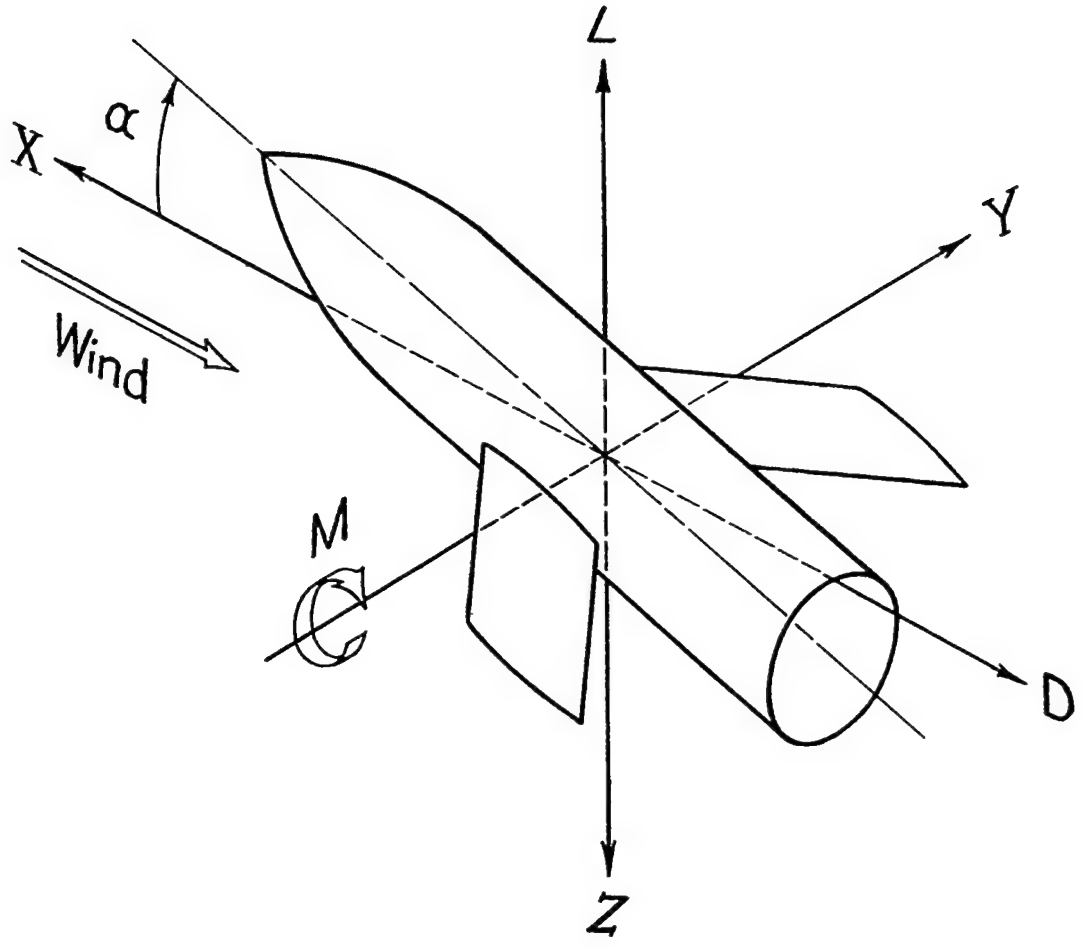

Figure 2.- System of stability axes. Positive values of forces, moments, and angles are indicated by arrows.

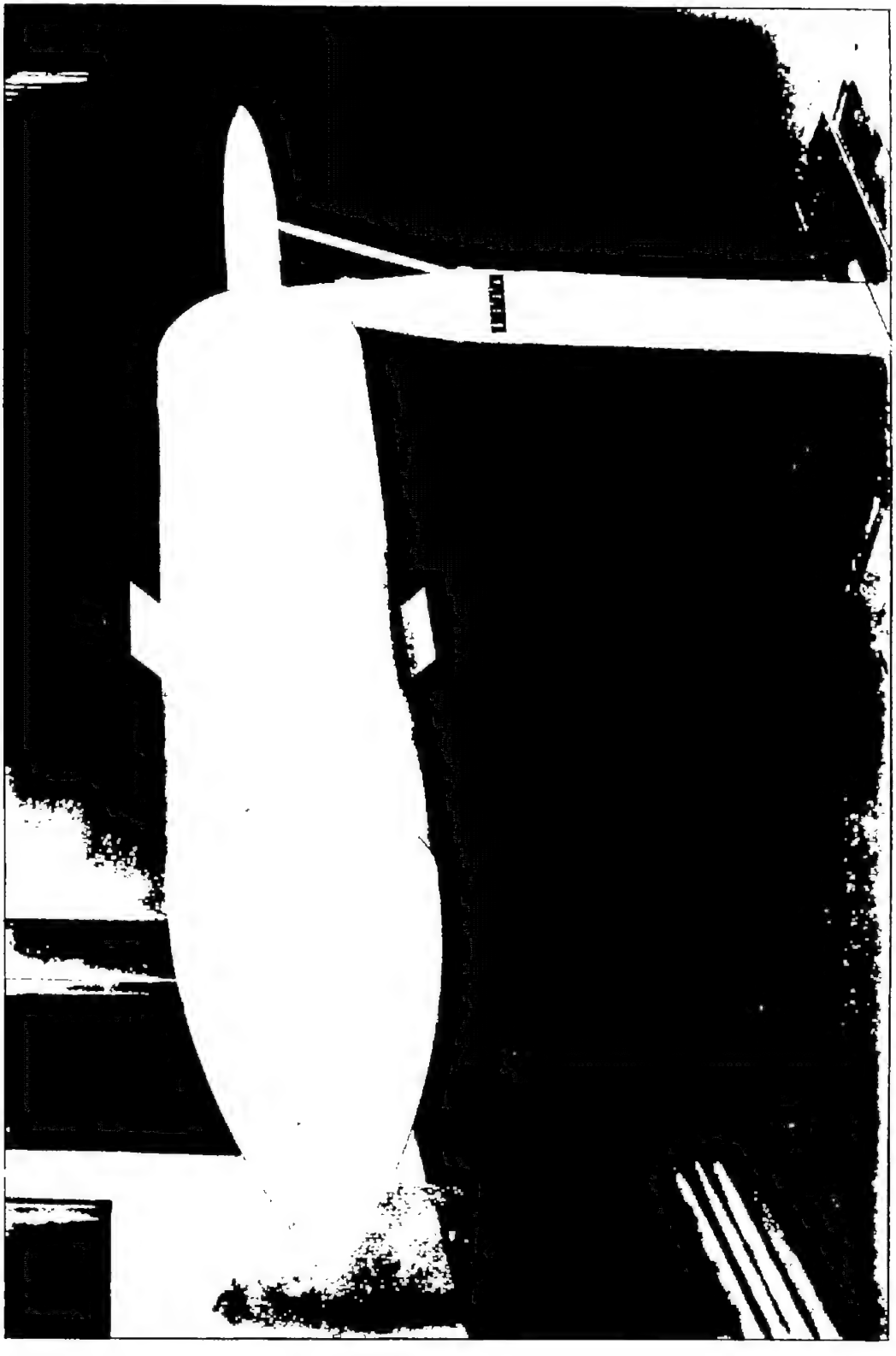

L-71321.1

Figure 3.- The D/b = 0.8 wing-body configuration mounted in the Langley 300 MPH 7- by 10-foot tunnel.

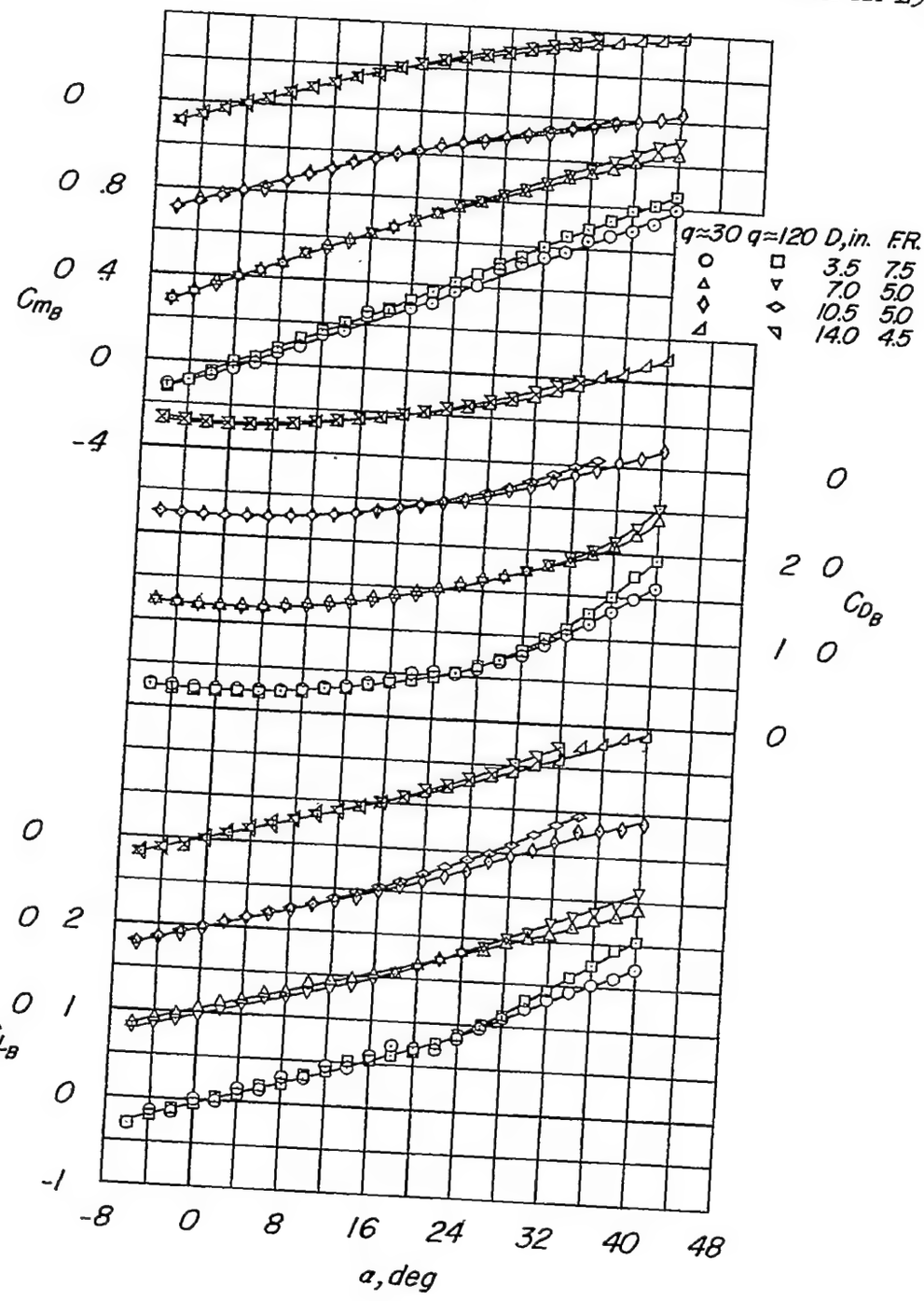

(a) Coefficients based on the body geometry. (C_m about 0.25$\bar{c}$ location of the large wing. See fig. 1.)

Figure 4.- Longitudinal aerodynamic characteristics of the body-alone configuration.

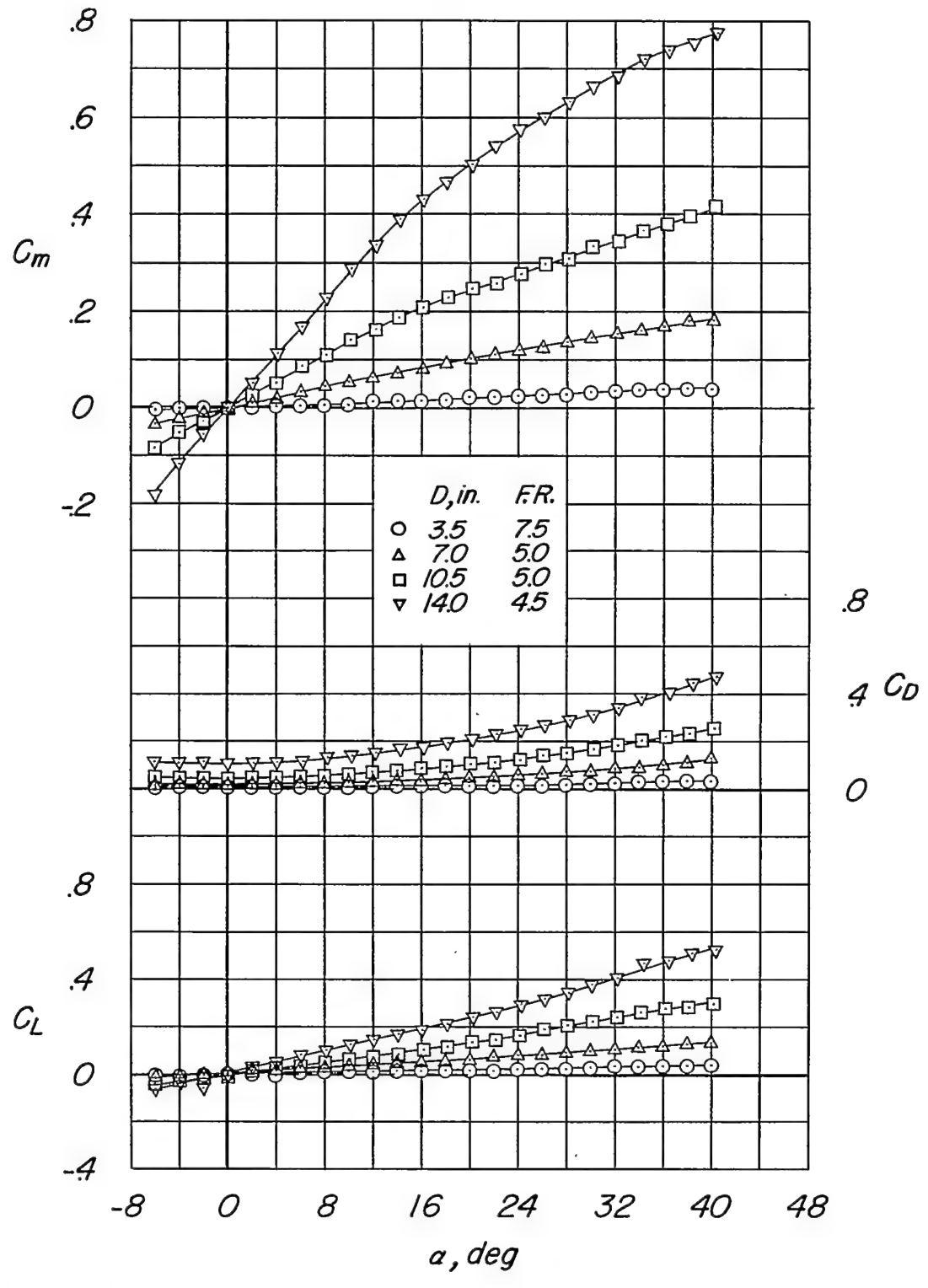

(b) Coefficients based on the geometry of the large wing. $q \approx 30$ lb/sq ft.

Figure 4.- Continued.

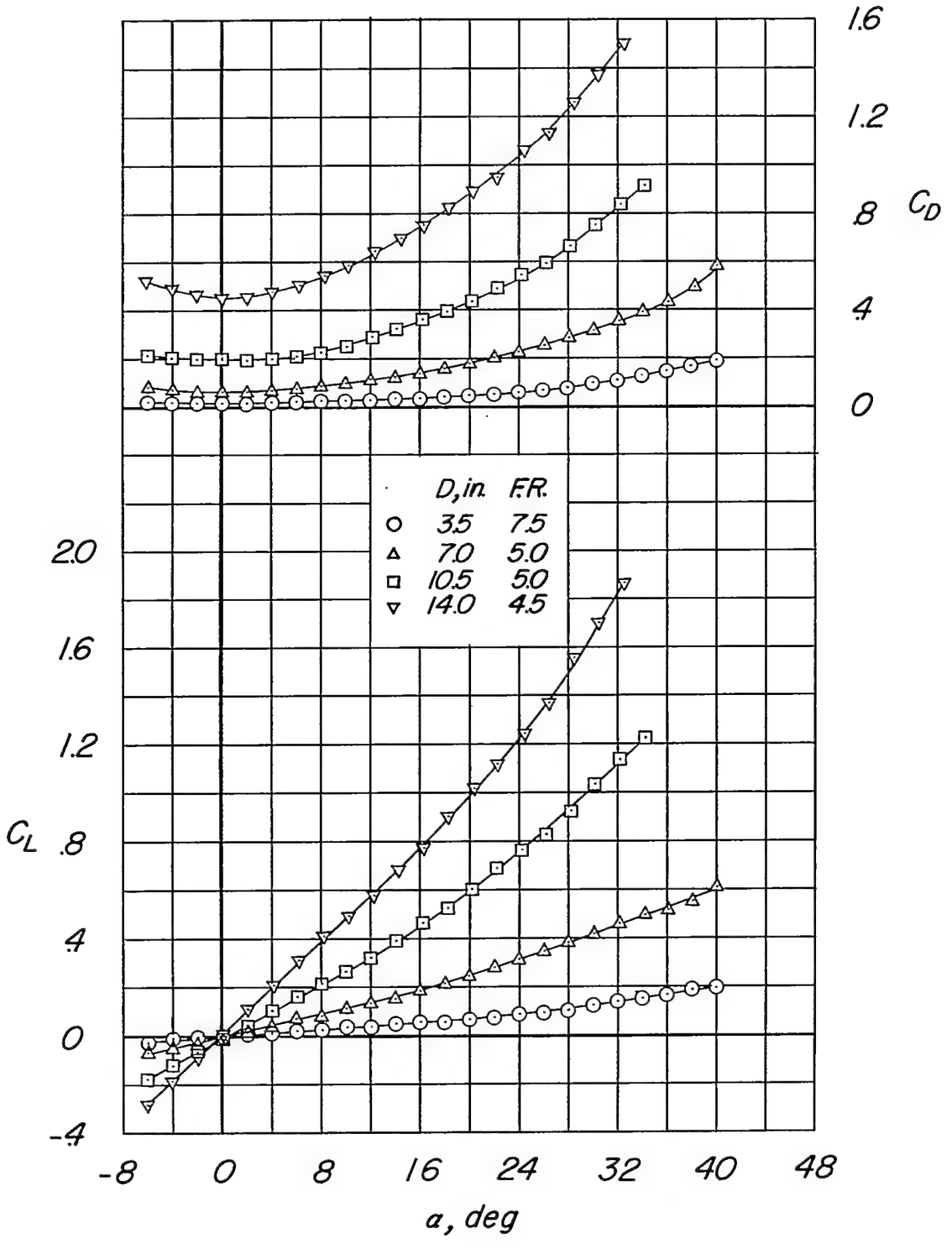

(c) Coefficients based on the geometry of the small wing. $q \approx 120$ lb/sq ft.

Figure 4.- Continued.

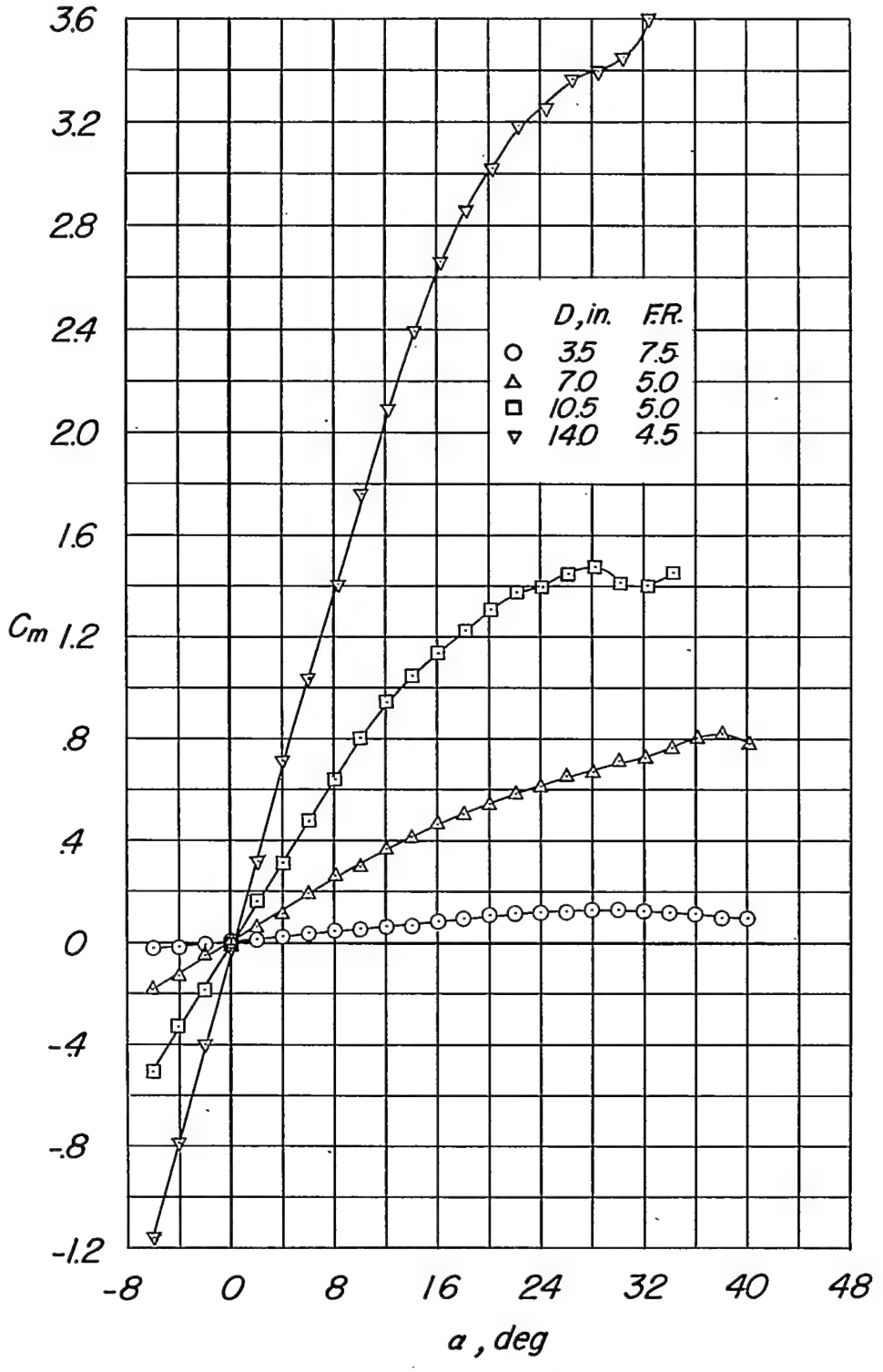

(c) Concluded.

Figure 4.- Concluded.

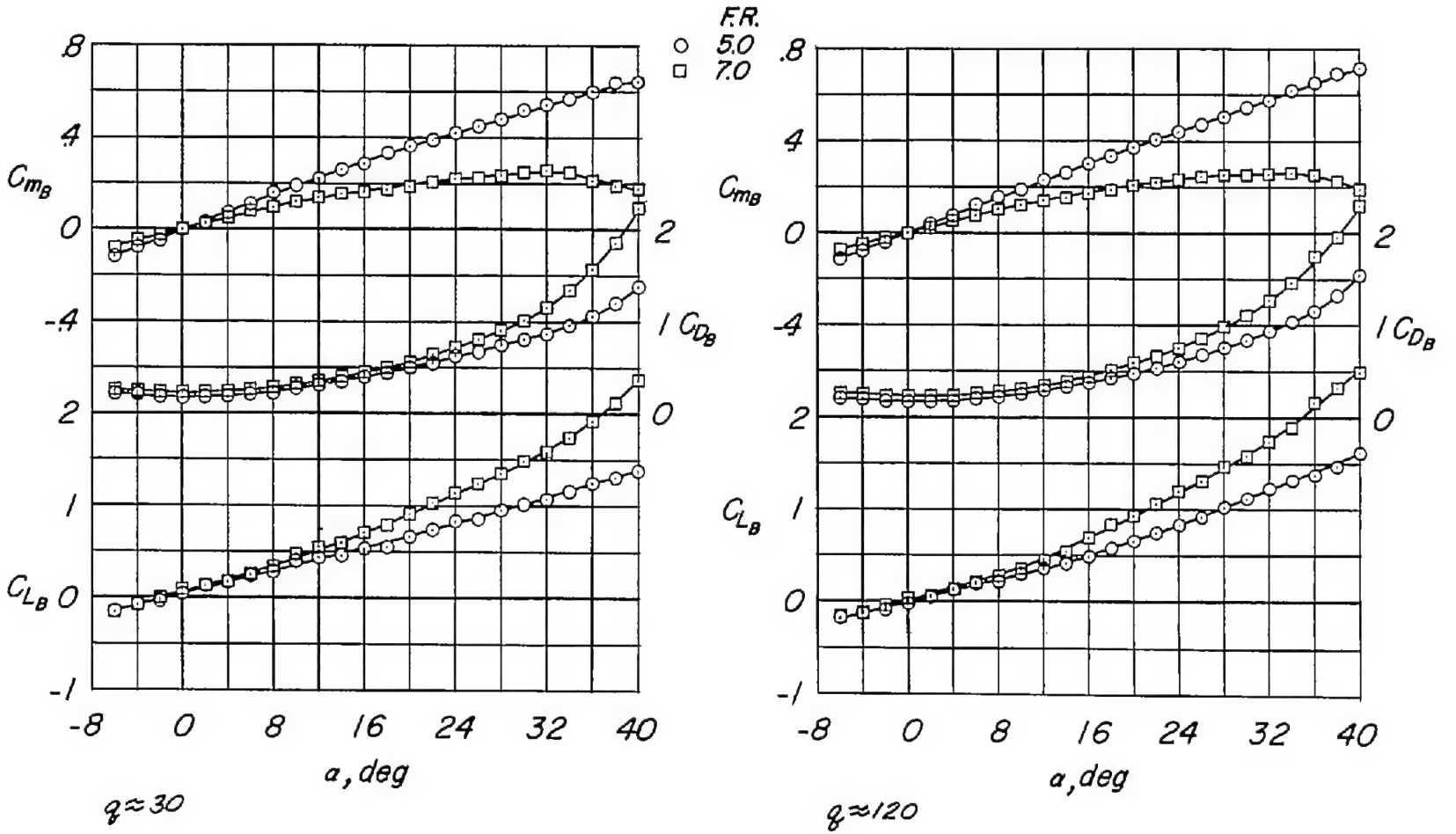

(a) Coefficients based on the body geometry. (C_m about 0.25$\bar{c}$ location of the large wing. See fig. 1.)

Figure 5.- Effect of body fineness ratio on the longitudinal aerodynamic characteristics of the body-alone configuration. D = 7.0 inch.

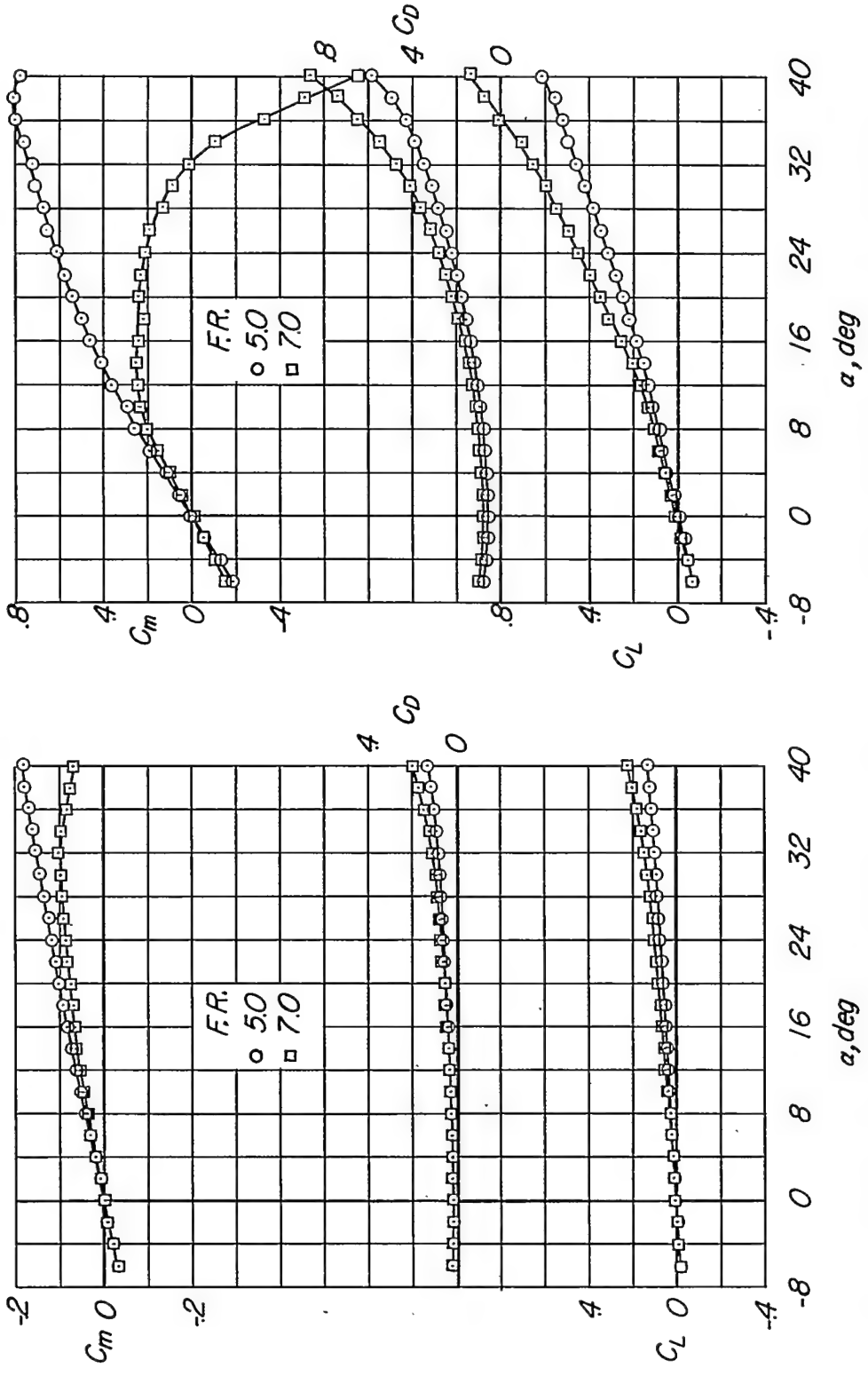

(b) Coefficients based on the geometry of the large wing. q ≈ 30 lb/sq ft.

(c) Coefficients based on the geometry of the small wing. q ≈ 120 lb/sq ft.

Figure 5.- Concluded.

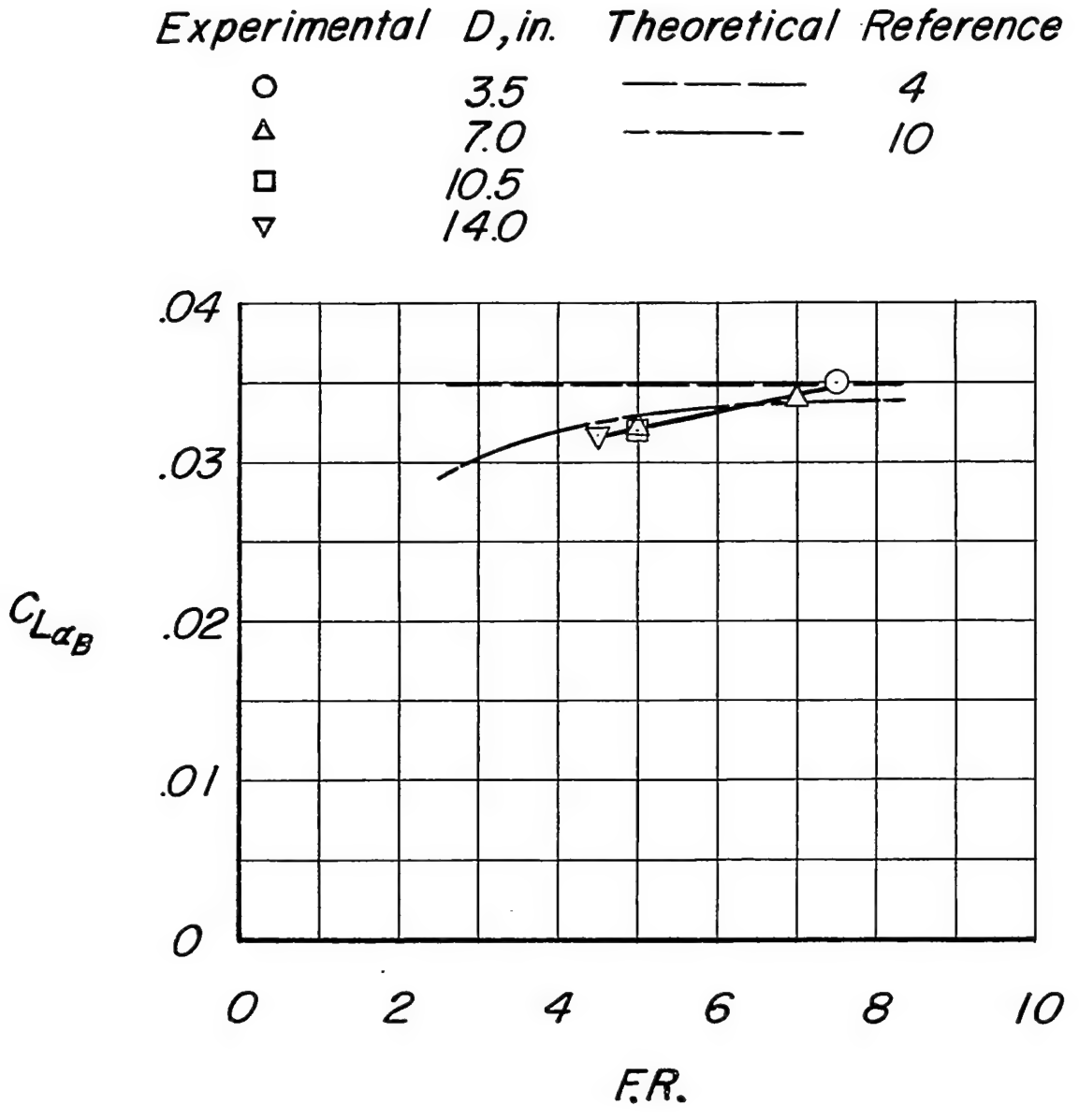

Figure 6.- Comparison with theory of the experimentally determined variation of $C_{L_{\alpha_B}}$ with body fineness ratio.

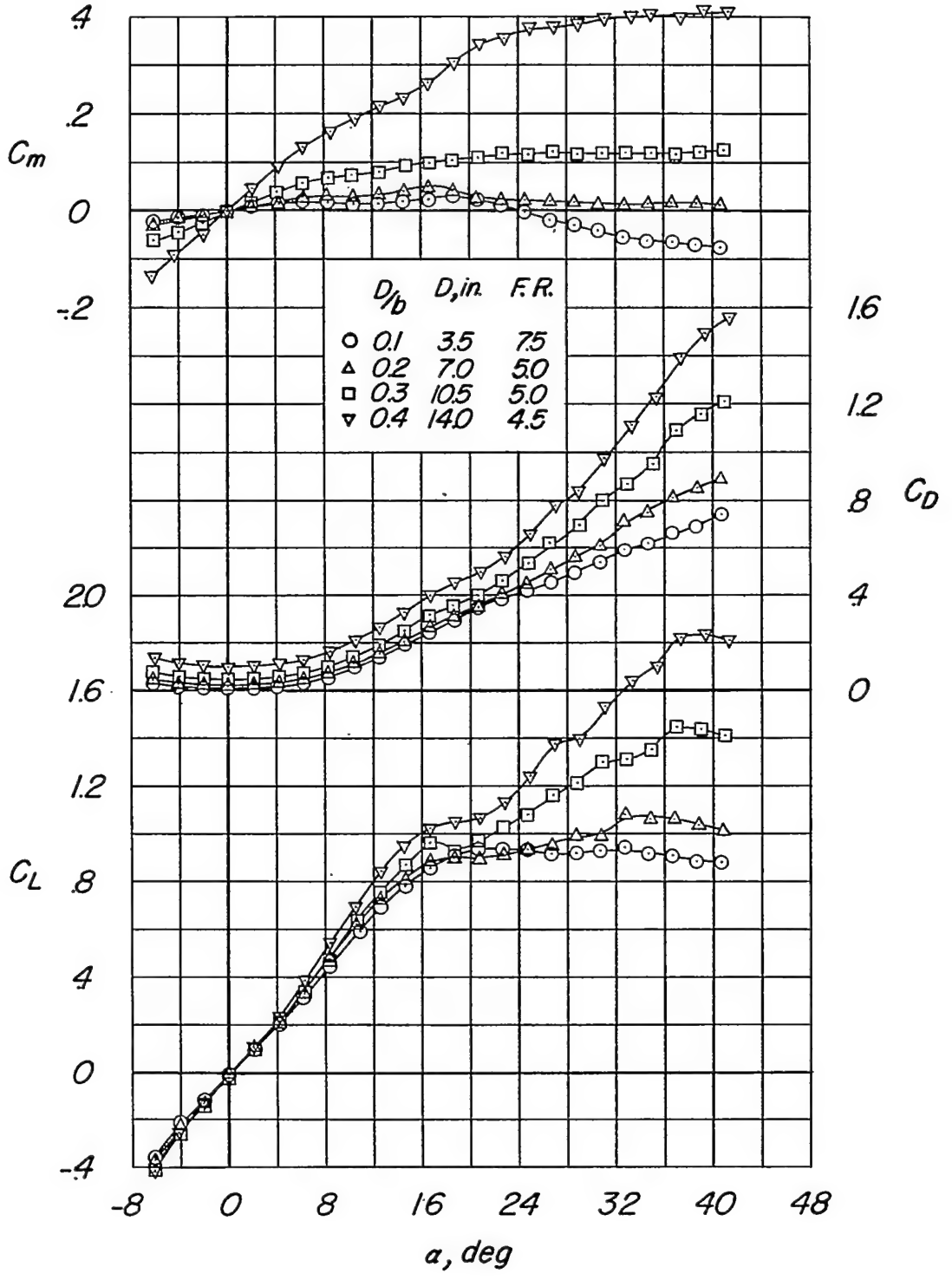

(a) Bodies with large wing. q ≈ 30 lb/sq ft.

Figure 7.- Longitudinal aerodynamic characteristics of the wing-body combinations.

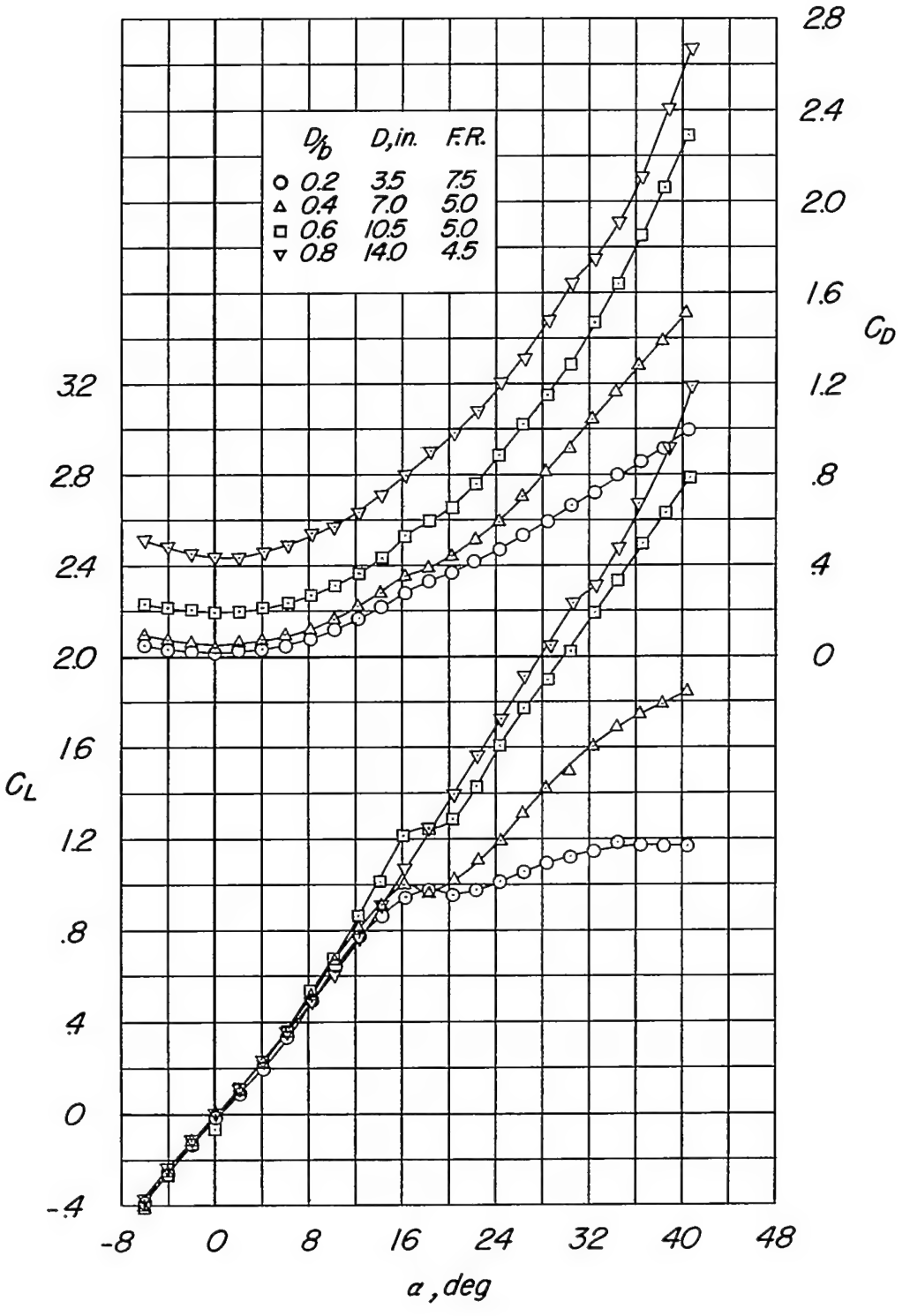

(b) Bodies with small wing. q ≈ 120 lb/sq ft.

Figure 7.- Continued.

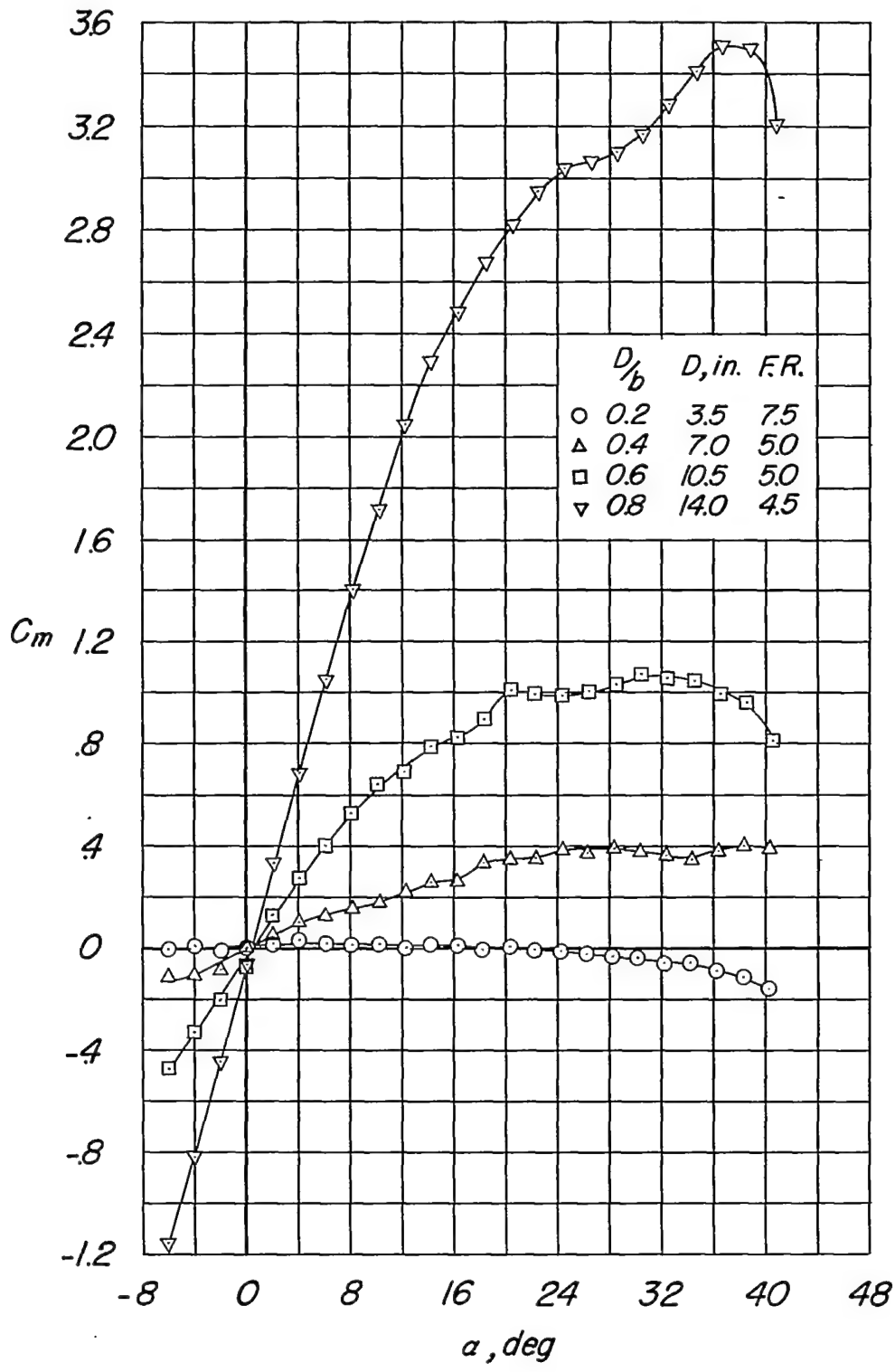

(b) Concluded.

Figure 7.- Concluded.

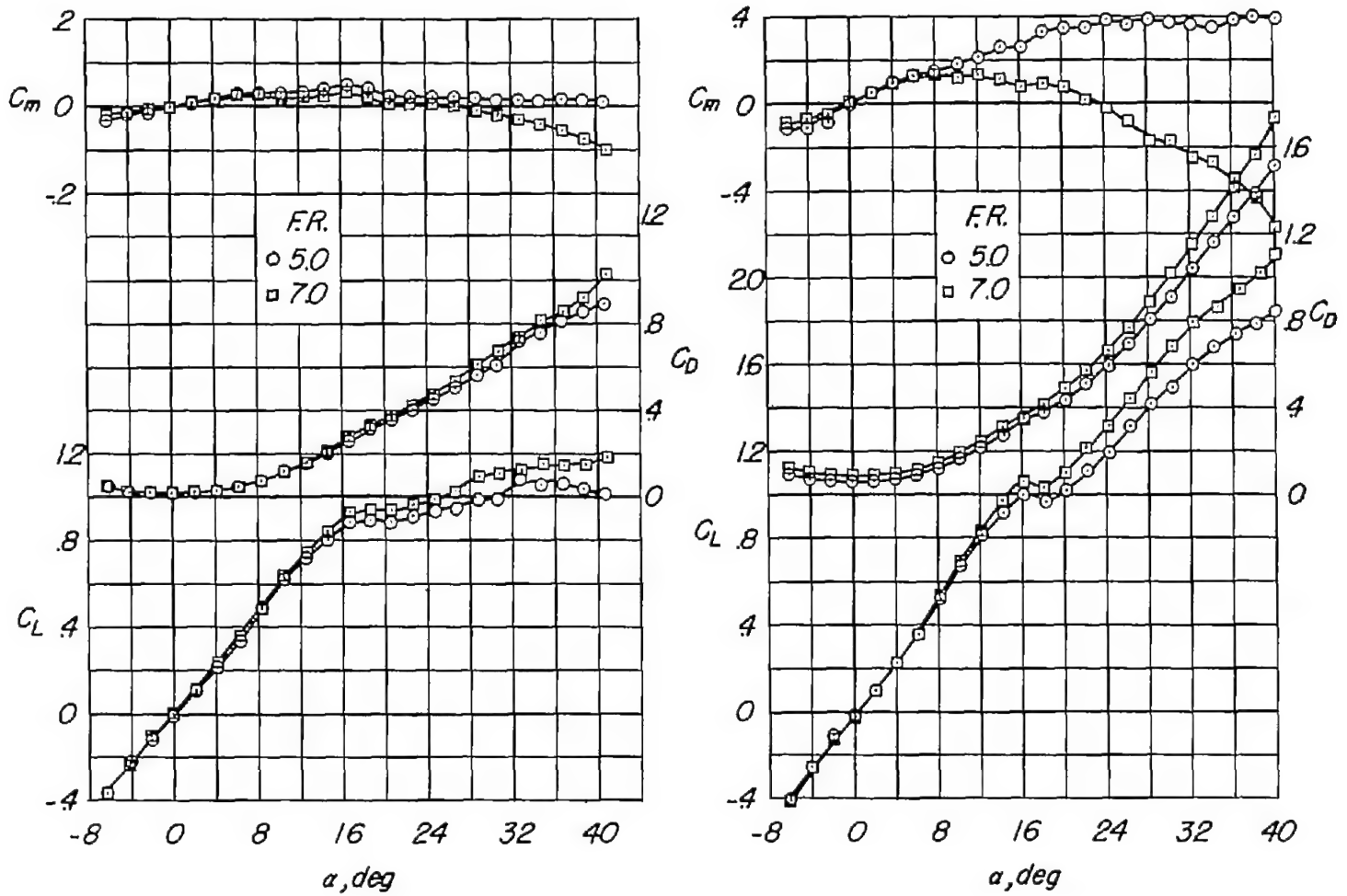

(a) Body with large wing. D/b = 0.2, q ≈ 30 lb/sq ft.

(b) Body with small wing. D/b = 0.4, q ≈ 120 lb/sq ft.

Figure 8.- Effect of body fineness ratio on the longitudinal aerodynamic characteristics of the wing-body combinations. D = 7.0 inch.

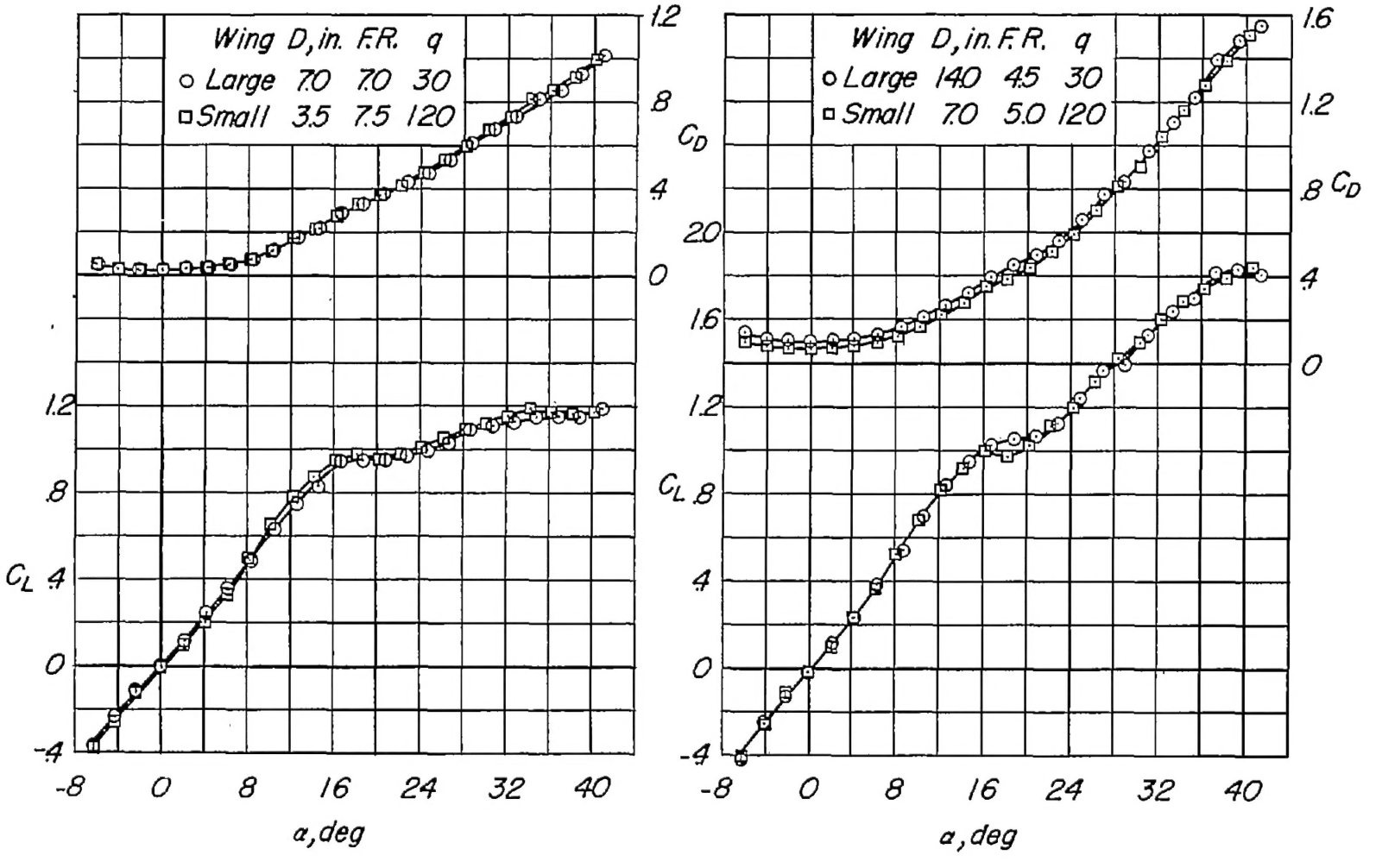

(a) D/b = 0.2.

(b) D/b = 0.4.

Figure 9.- Effect of wing size on the longitudinal aerodynamic characteristics of the wing-body combinations.

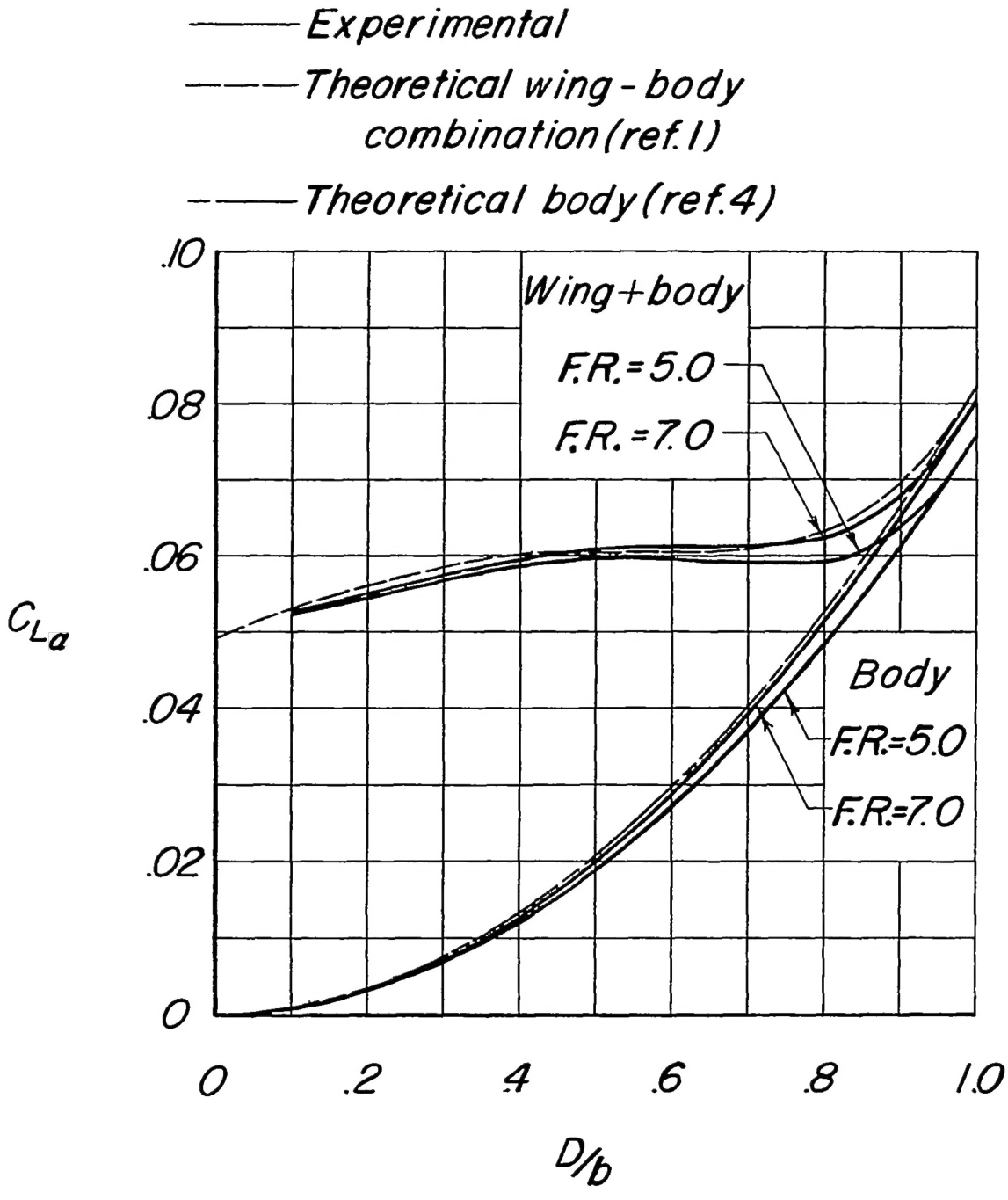

Figure 10.- Comparison with theory of the experimentally determined variation of C_{L_α} with D/b.

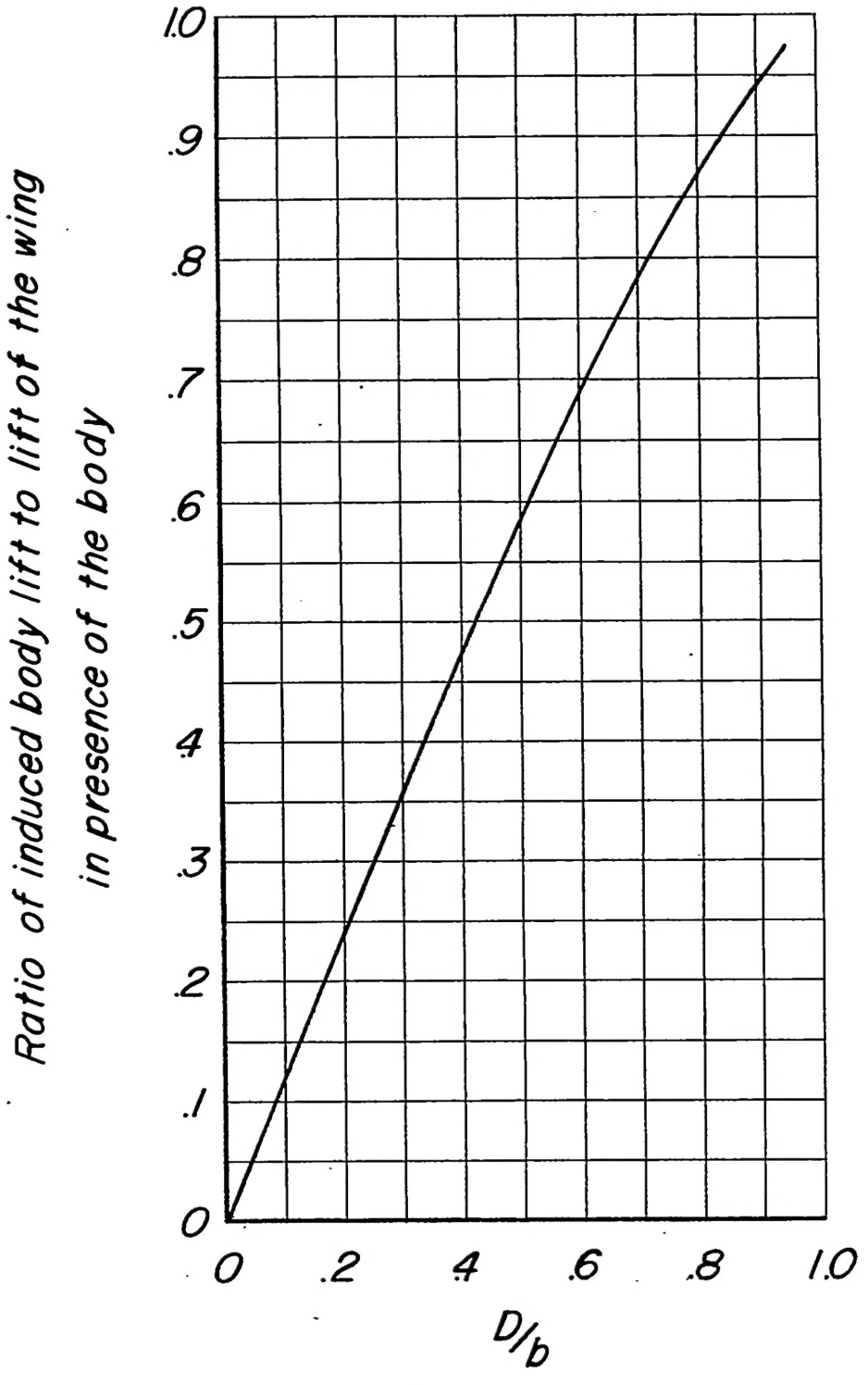

Figure 11.- Theoretical variation with D/b of the ratio of the lift induced on the body by the wing to the lift of the wing in the presence of the body (from ref. 4 or 9).

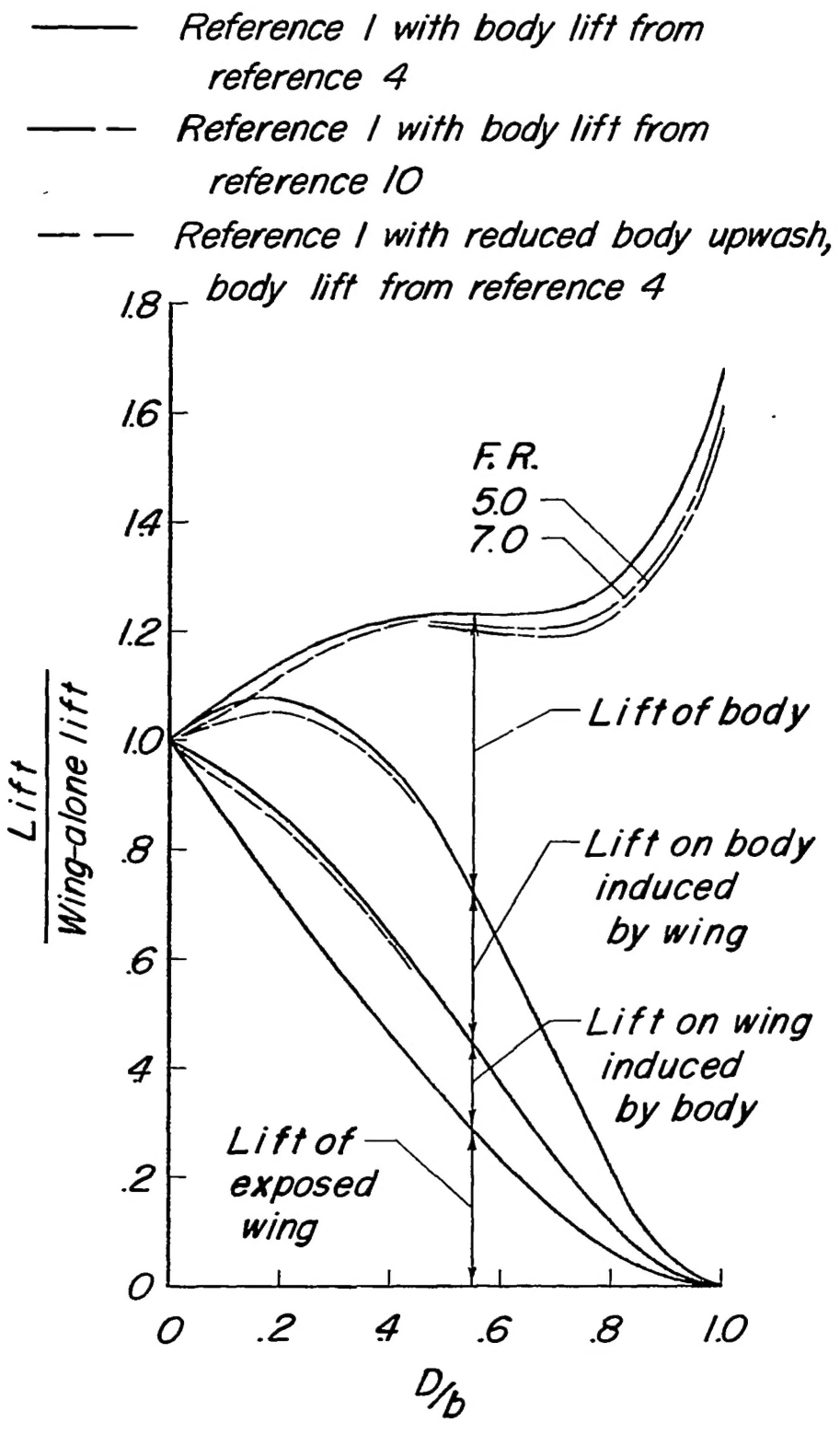

Figure 12.- Variation with D/b of the contributions to the lift of the wing-body configuration as determined by the method of reference 1.

NACA-Langley - 11-30-53 - 325